Published in final edited form as:
Cell Host Microbe. 2014 May 14; 15(5): 644–651. doi:10.1016/j.chom.2014.04.009.

Broadly neutralizing Influenza hemagglutinin stem– specific antibody CR8020 targets residues that are prone to escape due to host selection pressure

Kannan Tharakaraman[+], **Vidya Subramanian**[+], **David Cain**, **V. Sasisekharan**, and **Ram Sasisekharan**[*]
Department of Biological Engineering, Skolkovo-MIT Center for Biomedical Engineering, Singapore-MIT Alliance for Research and Technology, Koch Institute of Integrative Cancer Research, Massachusetts Institute of Technology, 77 Massachusetts Avenue, Cambridge MA 02139, USA

SUMMARY

Broadly neutralizing antibodies (bNAb) that target a conserved region of a viral antigen hold significant therapeutic promise. CR8020 is a bNAb that targets the stem region of influenza A virus (IAV) hemagglutinin (HA). CR8020 is currently being evaluated for prophylactic use against group 2 IAVs in phase II studies. Structural and computational analyses reported here indicate that CR8020 targets HA residues that are prone to antigenic drift and host selection pressure. Critically, CR8020 escape mutation is seen in certain H7N9 viruses from recent outbreaks. Furthermore, the ability of the bNAb Fc region to effectively engage activating Fcγ receptors (FCγR) is essential for antibody efficacy. In this regard, our data indicate that the membrane could sterically hinder the formation of HA-CR8020-FcγRIIa/HA-IgG-FcγRIIIa ternary complexes. Altogether, our analyses suggest that epitope mutability and accessibility to immune complex assembly are important attributes to consider when evaluating bNAb candidates for clinical development.

INTRODUCTION

Recently, technologies related to the characterization and isolation of B-cells from infected or vaccinated individuals have identified broadly neutralizing antibodies (bNAbs) targeting highly diverse pathogens, such as HIV (Zwick et al., 2003), (Wu et al., 2010), (Scheid et al., 2011), (Pejchal et al., 2010), (Pejchal et al., 2011), (Zwick et al., 2001) and influenza (Ekiert et al., 2011), (Sui et al., 2009), (Dreyfus et al., 2013), (Corti et al., 2011). Analysis of these antibodies, including the epitopes they target and their germline of origin, provides information useful to vaccine design (Kwong et al., 2011), (Nabel, 2012), (Steel et al., 2010). In addition, in the absence of the development of a universal, broadly protective

[*]to whom correspondence should be addressed: rams@mit.edu; ph: (617) 258 9494; fax: (617) 258 9494.
[+]Contributed equally;

Note Added in Proof

Since the submission of this manuscript, one of the CR8020 clinical trials (NCT01992276; http://clinicaltrials.gov/ct2/show/NCT01992276?term=cr8020&rank=4) was withdrawn due to “preliminary efficacy results from an influenza challenge trial”.

vaccine strategy for viral diseases such as influenza, passive immunization using antibodies could help treat the disease and protect so-called “at risk” populations, such as the immunocompromised and elderly individuals. While early bNAbs for HIV, such as 2F5 (Muster et al., 1993) and 4E10 (Zwick et al., 2001) exhibited polyreactivity and unusually short half-lives in phase I trials, passive immunization for influenza and HIV has progressed to the point that multiple antibodies are now entering human clinical trials.

In the case of influenza, efforts were made in the past to isolate cross-reactive bNAbs targeting the conserved, relatively sub-dominant epitopes of the virus (Graves et al., Virology 1983 and Okuno et al., JVI 1993). With advances in technologies, the recent years have seen a tremendous surge in the development of bNAbs against the hemagglutinin (HA) protein of influenza A virus (Ekiert et al., 2011), (Sui et al., 2009), (Dreyfus et al., 2013), (Corti et al., 2011). A bNAb targets a conserved region of the antigen and is thereby efficacious against a wide range of strains. The applicability of such bNAbs in a prophylactic setting is being evaluated for CR8020 (Ekiert et al., 2011), which targets group 2 influenza A viruses. Currently, CR8020 is evaluated both as a single agent (NCT01938352) and in combination with a group 1 bANb – CR6261 – (NCT01992276) in two separate Phase II studies. In these studies, the prophylactic potential of CR8020 is being evaluated in individuals who are infected with a group 2 H3N2 virus. At present, CR8020 is the most advanced anti-group 2 bNAb undergoing clinical trials. The H3N2 subtype has been circulating in humans since 1968, causing more than 400,000 deaths in the United States alone (Kawaoka et al., 1989), (Jansen et al., 2007), (Iwane et al., 2004). Besides H3N2, another group 2 subtype, the avian-origin H7N9, recently led to 144 cases of infection in China (Gao et al., 2013). Of these cases, 46 died (>30% mortality), raising concerns that the virus might change into a form that is more transmissible in humans. Further troubling is the fact that the recent H7N9 strains are resistant to M2 channel blockers and some strains are also displaying resistance to Tamiflu and Relenza (Hai et al., 2013). In light of the above, an understanding of the biological activity of CR8020, as well as clinical considerations, particularly against group 2 subtypes H3N2 and H7N9, becomes extremely important.

RESULTS

CR8020 binding residues on HA are susceptible to sequence drift and potential for escape mutations

CR8020 targets an immune-subdominant, relatively conserved membrane-proximal stem region of HA, thus preventing fusion and viral entry through: (1) inhibiting fusogenic conformational change and/or (2) inhibiting cleavage of HA0 by host proteases. Interestingly, Ekiert DC *et. al.* identified two CR8020 escape mutations – D19N and G33E in HA2 domain – which also occur in select natural H3 strains (Ekiert et al., 2011). In their study, the antibody was found to be less sensitive to other epitope changes observed in naturally occurring H3N2 strains. To identify the potential for escape mutations that are not readily observed in nature, we applied our novel computational approach, based on atomic interaction networks, to examine the relationship between amino acids within the epitope and to evaluate the mutability of the individual sites. A detailed description of the atomic

interaction network approach, called SIN (Significant Interactions Network), can be found elsewhere (Soundararajan et al., 2011). A brief description of the network approach can be found in the METHODS section.

Previously, we applied this approach to successfully demonstrate how immunologic, pressure-induced antigenic changes on the globular head region of A/Puerto Rico/8/1934 (PR8) H1N1 influenza A virus can affect host receptor-binding affinity through inter-residue interactions (Soundararajan et al., 2011). From sequence analyses, 9 out of 13 CR8020 epitope sites have seen amino acid variation (METHODS). Furthermore, SIN scores suggest that only four sites – R25, Q34, N146 and G150 – are under mutational constraints (SIN > 0.2), suggesting the potential for antiviral-associated escape mutations (METHODS and Table 1). Using the co-crystal structure of CR8020 Fab in complex with HA of A/Hong Kong/1/1968 (H3N2) (PDB: 3SDY), the mutable sites were analyzed, and HA mutations that contribute to destabilizing the epitope-paratope interface without affecting HA stability (METHODS) were predicted with atomic network interactions and verified with physics-based modeling functions (Table 1). Interestingly, the predicted escape mutations are a single base pair change away from the wild type sequence, implying potential for emergence of mutants that can escape antibody detection and neutralization. Similarly, analysis to determine potential escape mutations for H7 HA using a model of CR8020 docked with A/Shanghai/02/2013(H7N9) HA (PDB: 4LN3) yielded 16 mutations at 7 mutable sites (Table 2).

Changes in CR8020 binding residues may be driven by host selection pressure—Critically, the D19N CR8020 escape mutation is seen in one of the circulating H7N9 outbreak viruses – A/Wuxi/1/2013 (H7N9) – suggesting that CR8020 is likely to be even less effective against this recent outbreak virus. Notably, this mutation has not been previously observed in an Asian H7 virus. Out of the 612 H7 HA sequences available in the public database, 514 sequences (~84%) contain D at position 19, and 98 sequences (~16%) contain N. The fact that HA can acquire stem mutations begs the question whether these mutations are associated with antigenic drift and immune escape. Until recently, the immunodominance of the head region and the potency of antibodies directed to the head yielded the concept of the canonical antigenic site model of HA, wherein a majority of the antigenic sites are concentrated near the receptor binding site region (Soundararajan et al., 2011), (Gerhard et al., 1981), (Wiley et al., 1981), (Wilson et al., 1981), (Tsuchiya et al., 2001). However, recent vaccine clinical studies however have identified fusion-inhibiting stem binding bNAbs in humans (Hardelid et al., 2010), (Wei et al., 2010), antibodies which are more broadly reactive. Additionally, analyses of B-cell epitopes from the Immune Epitope Database (http://www.iedb.org) highlight the involvement of many HA2 stem residues, including amino acids within the CR8020 epitope, as part of many B-cell epitopes (Figure S1), indicating the ability of the stem region to induce protective response. To determine whether the D19N substitution is associated with antigenic drift, we considered accompanying changes within close spatial and temporal proximity (METHODS), as such co-evolving multiple mutations are probably indicative of immune pressure exerted by host antibodies. Interestingly, residues at 326 of HA1 and 160 of HA2 co-evolve along with site 19 of HA2 (Figure 1A–D). The spatial proximity of these sites (Figure 1E) and their co-

evolution are consistent with the changes observed at globular head B-cell epitopes of HA (Shih AC Proc Natl Acad Sci U S A. 2007 Apr 10;104(15):6283–8, Huang JW BMC Bioinformatics. 2009 Jan 30;10 Suppl 1:S41), implying stem antigenic evolution as a result of host selection pressure. It must be noted that the chance occurrence of such co-evolving sites in the stem region where mutation rates are low is highly unlikely. In this context, given the differences within the epitope for H7 compared to H3, we anticipate that CR8020 would bind with low affinity, a result which was verified experimentally. Whereas CR8020 bind with relatively high affinity to HA of H3N2 strains such as A/Brisbane/10/2007 (IC_{50} of 3.36 nM) and A/Wyoming/3/2003 (IC_{50} of 0.06 nM), CR8020 did not show binding to A/Shanghai/02/2013, a representative H7N9 strain (Figure 1F).

Membrane may sterically hinder binding of Fcγ R to Fc within the immune complex

In addition to mutability of the epitope, on the basis of a recent study by DiLillo DJ *et. al.* (Dilillo et al., 2014), another factor that could limit the efficacy of bNAbs is the ability of the Fc region of the antibody to effectively engage Fcγ receptors *in vivo*. This study compared the neutralization potential of head binding strain-specific HA antibodies against stem binding bNAbs and found that, although recognition of a “functional” epitope by the Fab arm of an antibody is pivotal for *in vitro* neutralization of the virus, the Fc-Fcγ interaction and activation of antibody dependent cellular cytotoxicity (ADCC) was critical for the *in vivo* efficacy of stem binding bNAbs. The Fc-Fcγ receptor interaction is key for regulating a host of innate and adaptive immune responses *in vivo*. Antibodies can engage both activating and inhibitory Fcγ receptors as well as mediate killing of infected cells expressing HA by ADCC through interaction with activating Fcγ receptors (FcγRIIa and FcγRIIIa). Given that CR8020 targets a membrane-proximal epitope (distance between base of the epitope and membrane is approximately 14A°), we assessed whether accessing the Fc-tail of the CR8020-HA immune complex could be an issue for the activating FcγRs. We evaluated the ability of IgG CR8020 to engage Fcγ receptors by building a molecular model of the activation complex of FcγRIIa/RcγIIIa in the liganded state (HA-CR8020 (IgG)) and, in turn, evaluated whether the viral or cellular membrane could sterically hinder with the complex (Figure 2A–D and METHODS). Both FcγRIIa and FcγRIIIa were chosen for this modeling analysis because these are the two common activating FcγRs in humans. Our structural modeling shows that the membrane could sterically hinder the formation of HA-CR8020-FcγRIIa and HA-CR8020-FcγRIIIa ternary complexes (Figure 2A–D). Because only one of the activating FcγRs (FcγRIIIa) can potentially engage with CR8020 (Figure 2B), this could possibly decrease the biological activity and potentially the clinical efficacy of the antibody, given that it is unclear which FcγR could dominate *in vivo*. A similar modeling exercise performed on a different stem-binding antibody, FI6, which binds higher up the stem region than CR8020, demonstrated that the antibody may have a higher potential to form the ternary complex with HA and both activating receptors, FcγRIIa/FcγRIIIa (data not shown). This is supported by the recent study, which showed that PR8 virus-FI6 immune complex efficiently binds to FcγRIIIa receptor (Dilillo et al., 2014). Furthermore, comparison of CR8020 to an antibody binding the trimeric interface indicates that CR8020 is ~10-fold less potent in eliciting ADCC, measured as either concentration of onset or fold-induction (Figure 2E). Altogether, the experimental data combined with the results of our modeling analyses indicate that location and mutability of the epitope could play critical

roles in determining the efficacy (or lack of) of CR8020 in the clinical setting. In most preclinical virus-challenge experiments, dosing of the antibody and the different strains of mice or ferrets is likely measuring the ability of the bNAbs to directly neutralize virus *in vivo*. However, the recent study published with humanized mice expressing human FcγR suggests that Fc-FcγR interactions do play a key role for at least two of the anti-stem bNAbs tested and that at higher doses the *in vivo* protection can be independent of the Fc-FcγR interaction (Dilillo et al., 2014). The Fc-FcγR interaction requirement is well established for antibodies that are used for other indications such as cancer. The results of our analyses have practical implications for designing human influenza clinical trials using bNAbs. Importantly, dosing regimen, Fc engineering (for maximum affinity towards activating FcγRs), and careful recruitment of patient population (keeping in mind FcγR polymorphism) need to be considered for clinical trial design.

DISCUSSION

In our modeling of the activation complex, the oligomeric state of FcγRIIa/FcγRIIa is kept as a monomer. Although it is believed that FcγRIIa is constitutively present as a dimer on the cell surface, the exact oligomeric state of FcγRIIa in the HA–IgG–FcγRIIa complex has not been characterized. Nevertheless, modeling the activation complex with the crystallographic dimer of FcγRIIa (source PDB: 1FCG) does not alter the results of our analysis (data not shown).

Dilillo DJ *et. al.*, suggest that conformational changes induced in the Fc upon binding to the epitope could be the reason for the difference in the ADCC potential of anti-stem mAbs in comparison to anti-head mAbs. Although our analysis does not take into consideration Fc conformational changes, the Fc:FcγR modeling analysis suggests that steric hindrance could also be a major factor in the differential FcγR engaging capacities. Although Dilillo DJ *et. al.*, demonstrated differences between anti-head mAbs versus anti-stem mAbs in their ability to engage FcRs, our analysis goes one step above to explain the striking differences in ADCC mediated cell killing between two anti-stem bNAbs.

In light of the limitations of CR8020 identified by this study and the importance of antiviral strategies against group 2 viruses such as H3N2 and H7N9, bNAbs that target epitopes that are accessible to immune complex assembly and less susceptible to mutations are desired. Generally, epitopes that are closer to the viral membrane harbor the most conserved and highly networked epitopes with broad spectrum neutralizing potential; however location of the epitope could impose constraints on accessibility. Conversely, epitopes on the globular head are accessible but are susceptible to rapid antigenic drift (Figure S2). Therefore, both epitope mutability and accessibility to immune complex assembly are important attributes to factor in as one evaluates suitable antibody candidates for clinical development.

Finally, we believe that these results have important ramifications for vaccine design. Multiple of the broadly neutralizing antibodies originate from the Vh1-69 germline (Friesen et al., 2014; Hwang et al., 2014). On the basis of the CR8020 data, strategies focused on activation of this germline may not be ideal to elicit full spectrum protection. Instead, activation of other germlines, such as Vh3–30, may provide a better solution.

EXPERIMENTAL PROCEDURES

Capturing network of protein residues (SIN)

The coordinates of A/X-31(H3N2) HA trimeric complex (PDB: 1HGG) and A/Shanghai/02/2013(H7N9) HA (PDB: 4LN3) were used to compute highly networked residues. For each case, various inter-residue inter-atomic contacts including putative hydrogen bonds (including water-bridged ones), disulfide bonds, pi-bonds, polar interactions, salt bridges, and Van der Waals interactions (non-hydrogen) occurring between pairs of residues were computed as described previously (Soundararajan et al., 2011). The data was assembled into an array of eight atomic interaction matrices. A weighted sum of the eight atomic interaction matrices was computed to produce a single matrix that accounts for the strength of atomic interaction between residue pairs, using weights derived from relative atomic interaction energies (Soundararajan et al., 2011). The inter-residue interaction network calculated in this fashion generates a matrix that describes all the contacts made between pairs of residues. Each element *i, j* is the sum of the path scores of all paths between residues *i* and *j*. The degree of networking score for each residue was computed by summing across the rows of the matrix, which corresponds to the extent of "networking" for each residue. The degree of networking score was normalized (SIN score) with the maximum score for the protein so that the scores varied from 0 (absence of any network) to 1 (most networked). From the previous study, residues with a SIN score ranging from 0 to 0.2 are considered poorly networked, those with 0.2–0.5 are considered moderately networked, and those with >0.5 are highly networked.

Sequences, amino acid variation and computation of coevolving residues

17,921 sequences of the H3N2 HA of human, avian and swine H3N2 strains isolated between 1934 and 2014 were downloaded from fludb.org. From this, laboratory sequences, especially mutants, were excluded. If multiple sequences were present for the same strain, only the consensus was included. Additionally, only sequences that have complete coding regions including start and stop codons were considered. The above procedure yielded 3,794 full-length, non-redundant sequences. A similar procedure when applied to human, avian and swine H7N9 HA yielded 612 full-length, non-redundant sequences. The sequences were aligned using MUSCLE (Edgar, 2004). Then, we computed the extent of variation at each position with the SNP tool at fludb.org. From the alignment, intramolecular co-evolving residues were computed with the CAPS server using default parameters (http://bioinf.gen.tcd.ie/caps/home.html).

Computational prediction of H3 & H7 escape mutations with CR8020-HA co-crystal structures

Mutations detrimental to the epitope-paratope interface were first computed with a built-in binding energy scoring function in Discovery Studio, which performs amino-acid scanning mutagenesis on a set of selected epitope residues and evaluates the effect of single-point mutations on the binding affinity of molecular partners. Then, to assess whether a mutation can impact the stability of HA, the inter-residue interactions were computed upon modeling that residue on HA. A mutation is considered to be harmless if it maintains the inter-residue interaction network (determined by SIN) similar to that of the wild type.

Modeling the HA-IgG-FcγRIIa/HA-IgG-FcγRIIIa ternary activation complex

The modeling was carried out in two steps. In step one, the Fab arm of a human IgG1 (from X-ray crystal structure PDB: 1HZH) was superposed onto the CR8020-HA co-crystal structure (PDB: 3SDY). Because *Fab* and *Fab'* are positioned differently relative to the Fc, two different models of IgG-HA interactions were obtained. In step two, the FcγRIIa receptor from PDB: 3RY6 and FcγRIIIa receptor from PDB: 3AY4 were docked against the Fc by superposing the Fc:FcγRIIa/Fc:FcγRIIIa co-crystal structure on the Fc region of the IgG-HA complex. A similar procedure was carried out to obtain the HA-FI6-FcγRIIa/Fc:FcγRIIIa ternary activation complex. Structural alignment and visualization were performed with PyMOL.

ELISA binding assays

Recombinant hemagglutinin (Protein Sciences Corporation) was coated on 96-well microtiter plates (Immuno™ Maxisorp, Nunc) and blocked with 5% Blotto (Santa Cruz Biotechnology) in 1x PBS. Serially-diluted CR8020 antibody, whose sequence is described in patent PCT/EP2010/056217 (Throsby, 2010), was added, and binding detected using horseradish-peroxidase-conjugated goat anti-human IgG (Fc specific) (Bethyl Labs) followed by development with 3,3,5,5- tetramethylbenzidine solution (KPL). The absorbance at 450 nm was measured using a Spectramax plate reader (Molecular Devices) and data analyzed with the Softmax software.

Measurement of Antibody-Dependent Cellular Cytotoxicity

CR8020 and an antibody targeting the trimeric interface were tested for their ability to mediate FcγRIIIa engagement. Target cells were created by infecting A549 cells with A/Victoria/3/75 (H3N2) at a multiplicity of infection ~1.0 for 18 hours, after which cells are seeded into a white 96-well plate. Control experiments employing fluorescence-activated cell sorting indicated that both antibodies bound to infected cells. The ADCC Reporter Assay from Promega was used to assess killing with an assay control of an anti-CD20 mAb added to WIL2-S cells. Dilutions of "Test" & "Control" mAbs were added to Target cells, and engineered effector cells (Jurkat T-cells transfected with CD16 (V/V 158 variant) and NFAT-Firefly Luciferase Gene) are added to wells and allowed to incubate for 6 hours at 37°C. Then, Bio-GLO Luciferase substrate solution was added to wells in order to measure activation of FcγRIIIa and results read on a luminometer.

Supplementary Material

Refer to Web version on PubMed Central for supplementary material.

Acknowledgments

This work was funded in part by National Institutes of Health Merit Award (R37 GM057073-13), National Research Foundation supported Interdisciplinary Research group in Infectious Diseases of SMART (Singapore MIT alliance for Research and Technology) and the Skolkovo Foundation supported Infectious Diseases Center at MIT.

References

Corti D, Voss J, Gamblin SJ, Codoni G, Macagno A, Jarrossay D, Vachieri SG, Pinna D, Minola A, Vanzetta F, et al. A neutralizing antibody selected from plasma cells that binds to group 1 and group 2 influenza A hemagglutinins. Science. 2011; 333:850–856. [PubMed: 21798894]

Dilillo DJ, Tan GS, Palese P, Ravetch JV. Broadly neutralizing hemagglutinin stalk-specific antibodies require FcgammaR interactions for protection against influenza virus in vivo. Nat Med. 2014; 20:143–151. [PubMed: 24412922]

Dreyfus C, Ekiert DC, Wilson IA. Structure of a classical broadly neutralizing stem antibody in complex with a pandemic H2 influenza virus hemagglutinin. J Virol. 2013; 87:7149–7154. [PubMed: 23552413]

Edgar RC. MUSCLE: multiple sequence alignment with high accuracy and high throughput. Nucleic Acids Res. 2004; 32:1792–1797. [PubMed: 15034147]

Ekiert DC, Friesen RH, Bhabha G, Kwaks T, Jongeneelen M, Yu W, Ophorst C, Cox F, Korse HJ, Brandenburg B, et al. A highly conserved neutralizing epitope on group 2 influenza A viruses. Science. 2011; 333:843–850. [PubMed: 21737702]

Friesen RH, Lee PS, Stoop EJ, Hoffman RM, Ekiert DC, Bhabha G, Yu W, Juraszek J, Koudstaal W, Jongeneelen M, et al. A common solution to group 2 influenza virus neutralization. Proceedings of the National Academy of Sciences of the United States of America. 2014; 111:445–450. [PubMed: 24335589]

Gao R, Cao B, Hu Y, Feng Z, Wang D, Hu W, Chen J, Jie Z, Qiu H, Xu K, et al. Human infection with a novel avian-origin influenza A (H7N9) virus. N Engl J Med. 2013; 368:1888–1897. [PubMed: 23577628]

Gerhard W, Yewdell J, Frankel ME, Webster R. Antigenic structure of influenza virus haemagglutinin defined by hybridoma antibodies. Nature. 1981; 290:713–717. [PubMed: 6163993]

Hai R, Schmolke M, Leyva-Grado VH, Thangavel RR, Margine I, Jaffe EL, Krammer F, Solorzano A, Garcia-Sastre A, Palese P, et al. Influenza A(H7N9) virus gains neuraminidase inhibitor resistance without loss of in vivo virulence or transmissibility. Nat Commun. 2013; 4:2854. [PubMed: 24326875]

Hardelid P, Andrews NJ, Hoschler K, Stanford E, Baguelin M, Waight PA, Zambon M, Miller E. Assessment of baseline age-specific antibody prevalence and incidence of infection to novel influenza A/H1N1 2009. Health Technol Assess. 2010; 14:115–192. [PubMed: 21208549]

Hwang KK, Trama AM, Kozink DM, Chen X, Wiehe K, Cooper AJ, Xia SM, Wang M, Marshall DJ, Whitesides J, et al. IGHV1-69 B Cell Chronic Lymphocytic Leukemia Antibodies Cross-React with HIV-1 and Hepatitis C Virus Antigens as Well as Intestinal Commensal Bacteria. PloS one. 2014; 9:e90725. [PubMed: 24614505]

Iwane MK, Edwards KM, Szilagyi PG, Walker FJ, Griffin MR, Weinberg GA, Coulen C, Poehling KA, Shone LP, Balter S, et al. Population-based surveillance for hospitalizations associated with respiratory syncytial virus, influenza virus, and parainfluenza viruses among young children. Pediatrics. 2004; 113:1758–1764. [PubMed: 15173503]

Jansen AG, Sanders EA, Hoes AW, van Loon AM, Hak E. Influenza- and respiratory syncytial virus-associated mortality and hospitalisations. Eur Respir J. 2007; 30:1158–1166. [PubMed: 17715167]

Kawaoka Y, Krauss S, Webster RG. Avian-to-human transmission of the PB1 gene of influenza A viruses in the 1957 and 1968 pandemics. J Virol. 1989; 63:4603–4608. [PubMed: 2795713]

Kwong PD, Mascola JR, Nabel GJ. Rational design of vaccines to elicit broadly neutralizing antibodies to HIV-1. Cold Spring Harb Perspect Med. 2011; 1:a007278. [PubMed: 22229123]

Muster T, Steindl F, Purtscher M, Trkola A, Klima A, Himmler G, Ruker F, Katinger H. A conserved neutralizing epitope on gp41 of human immunodeficiency virus type 1. J Virol. 1993; 67:6642–6647. [PubMed: 7692082]

Nabel GJ. Rational design of vaccines for AIDS and influenza. Trans Am Clin Climatol Assoc. 2012; 123:9–15. discussion 15–16. [PubMed: 23303965]

Pejchal R, Doores KJ, Walker LM, Khayat R, Huang PS, Wang SK, Stanfield RL, Julien JP, Ramos A, Crispin M, et al. A potent and broad neutralizing antibody recognizes and penetrates the HIV glycan shield. Science. 2011; 334:1097–1103. [PubMed: 21998254]

Pejchal R, Walker LM, Stanfield RL, Phogat SK, Koff WC, Poignard P, Burton DR, Wilson IA. Structure and function of broadly reactive antibody PG16 reveal an H3 subdomain that mediates potent neutralization of HIV-1. Proc Natl Acad Sci U S A. 2010; 107:11483–11488. [PubMed: 20534513]

Scheid JF, Mouquet H, Ueberheide B, Diskin R, Klein F, Oliveira TY, Pietzsch J, Fenyo D, Abadir A, Velinzon K, et al. Sequence and structural convergence of broad and potent HIV antibodies that mimic CD4 binding. Science. 2011; 333:1633–1637. [PubMed: 21764753]

Soundararajan V, Zheng S, Patel N, Warnock K, Raman R, Wilson IA, Raguram S, Sasisekharan V, Sasisekharan R. Networks link antigenic and receptor-binding sites of influenza hemagglutinin: mechanistic insight into fitter strain propagation. Sci Rep. 2011; 1:200. [PubMed: 22355715]

Steel J, Lowen AC, Wang TT, Yondola M, Gao Q, Haye K, Garcia-Sastre A, Palese P. Influenza virus vaccine based on the conserved hemagglutinin stalk domain. MBio. 2010; 1

Sui J, Hwang WC, Perez S, Wei G, Aird D, Chen LM, Santelli E, Stec B, Cadwell G, Ali M, et al. Structural and functional bases for broad-spectrum neutralization of avian and human influenza A viruses. Nat Struct Mol Biol. 2009; 16:265–273. [PubMed: 19234466]

Throsby, MF.; Robert, Heinz Edward; Kwaks, Theodorus Hendrikus Jacobus; Jongeneelen, Mandy Antonia Catharina. Human binding molecules capable of neutralizing influenza virus H3N2 and uses thereof. Crucell Holland B.V.; Leiden (NL): 2010.

Tsuchiya E, Sugawara K, Hongo S, Matsuzaki Y, Muraki Y, Li ZN, Nakamura K. Antigenic structure of the haemagglutinin of human influenza A/H2N2 virus. J Gen Virol. 2001; 82:2475–2484. [PubMed: 11562540]

Wei CJ, Boyington JC, McTamney PM, Kong WP, Pearce MB, Xu L, Andersen H, Rao S, Tumpey TM, Yang ZY, et al. Induction of broadly neutralizing H1N1 influenza antibodies by vaccination. Science. 2010; 329:1060–1064. [PubMed: 20647428]

Wiley DC, Wilson IA, Skehel JJ. Structural identification of the antibody-binding sites of Hong Kong influenza haemagglutinin and their involvement in antigenic variation. Nature. 1981; 289:373–378. [PubMed: 6162101]

Wilson IA, Skehel JJ, Wiley DC. Structure of the haemagglutinin membrane glycoprotein of influenza virus at 3 A resolution. Nature. 1981; 289:366–373. [PubMed: 7464906]

Wu X, Yang ZY, Li Y, Hogerkorp CM, Schief WR, Seaman MS, Zhou T, Schmidt SD, Wu L, Xu L, et al. Rational design of envelope identifies broadly neutralizing human monoclonal antibodies to HIV-1. Science. 2010; 329:856–861. [PubMed: 20616233]

Zwick MB, Labrijn AF, Wang M, Spenlehauer C, Saphire EO, Binley JM, Moore JP, Stiegler G, Katinger H, Burton DR, et al. Broadly neutralizing antibodies targeted to the membrane-proximal external region of human immunodeficiency virus type 1 glycoprotein gp41. J Virol. 2001; 75:10892–10905. [PubMed: 11602729]

Zwick MB, Parren PW, Saphire EO, Church S, Wang M, Scott JK, Dawson PE, Wilson IA, Burton DR. Molecular features of the broadly neutralizing immunoglobulin G1 b12 required for recognition of human immunodeficiency virus type 1 gp120. J Virol. 2003; 77:5863–5876. [PubMed: 12719580]

HIGHLIGHTS

- HA residues targeted by the CR8020 antibody are susceptible to host selection pressure
- Influenza HA mutations have the potential to negatively impact CR8020 activity
- Known CR8020 escape mutation is found in at least one H7N9 outbreak virus
- Membrane may sterically hinder FcγR binding to Fc within the HA-CR8020 immune complex

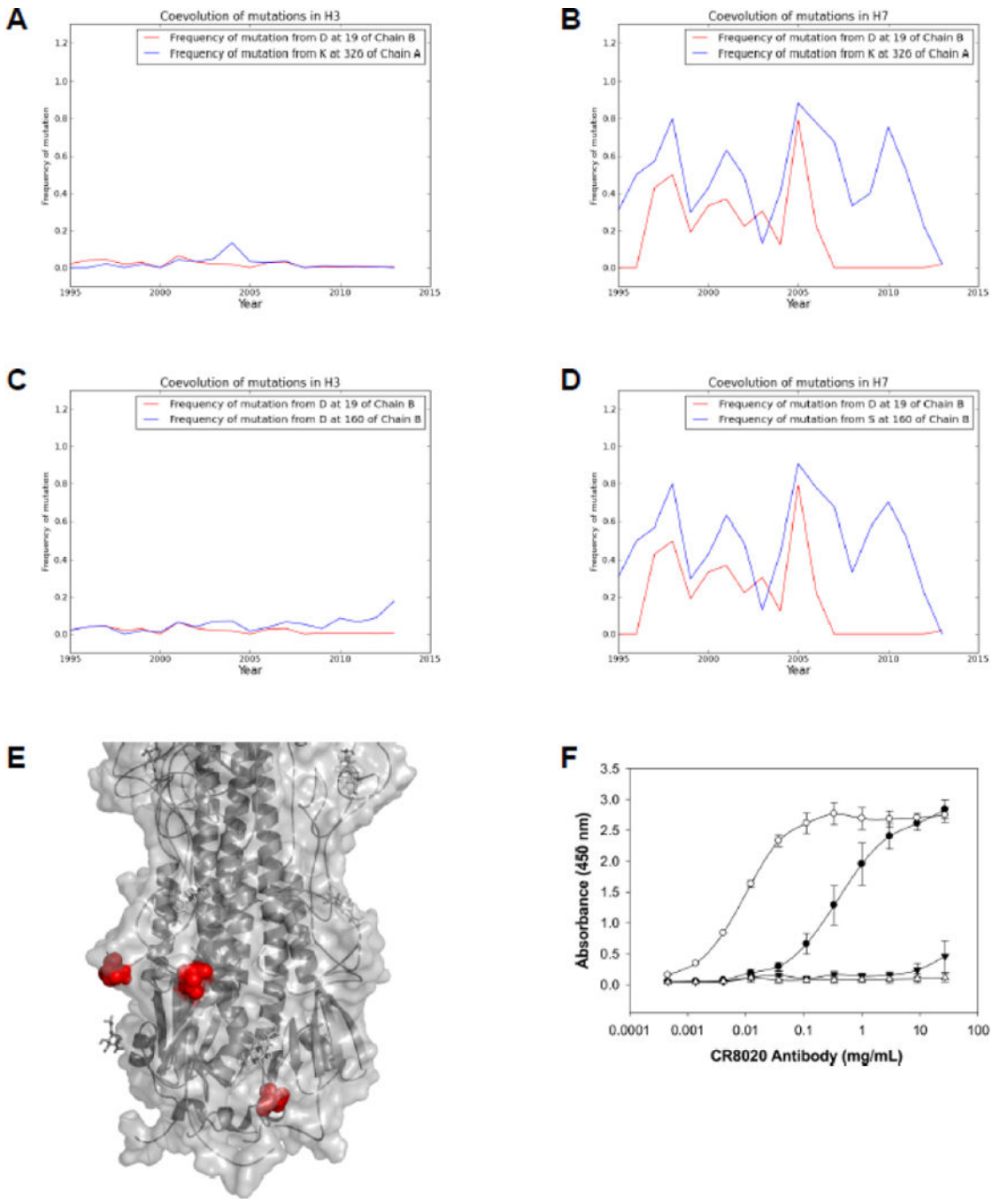

Figure 1. Coevolution of stem residues and measurement of CR8020 binding to various H3 and H7 strains

(A–D) Coevolution between residues at 19 (HA2) and 326 (HA1) in H3 and H7 are shown in **A** & **B**, respectively, and coevolution between residues at 19 (HA2) and 160 (HA2) in H3 and H7 are shown in **C** & **D**, respectively. In the alignment of 3,794 H3 sequences, the amino acid at position 19 of HA2 is conserved at 98.91% as aspartic acid (83.93% conservation in 612 H7 sequences). When aspartic acid at 19 mutates to asparagine, mutations occur in structurally proximal positions, referred as co-evolution. A similar trend

is observed in H7 subtype also. The frequency of mutation (instances of deviance from the conserved residue) as observed year-by-year in reported H3 and H7 sequences is demonstrated. A frequency of 0.0 means the position was entirely conserved in all sequences from that year, and frequency of 1.0 means that all sequences from that year possessed a mutation at the given position. Mutation frequency charts show the temporal covariance of the co-evolving residues. **(E)** Location of the coevolving residues on the stem region of HA. The main chain of HA (PDB: 1HGG), colored in gray, is shown in cartoon format, and the solvent accessible surface shown in transparency. The side chain atoms of the co-evolving residues are represented by spheres (red). All the images in the manuscript were rendered in PyMOL. (**F**) The ability for CR8020 to bind to influenza HA was measured, (○) H3N2 (A/Wyoming/3/2003); (●) H3N2 (A/Brisbane/10/2007); and (▼) H7N9 (A/Shanghai/02/2013). Also included was a BSA control (Δ), coated instead of hemagglutinin to ensure no non-specific binding. Figure 1F are the result of a representative experiment. The full binding curve was completed three times and an apparent Kd expressed as an average + standard deviation was determined. CR8020 bound A/Wyoming/3/2003 (H3N2) very strongly with an apparent Kd of approximately 60 pm (individual measurements of 57, 59, and <80 pM). CR8020 bound A/Brisbane/10/2007 (H3N2) with an apparent Kd of 3.36 + 1.97 nM. Binding to H7N9 A/Shanghai/02/2013 (H7N9) and A/Anhui/1/2013 (H7N9) was too weak in this assay to determine an apparent Kd. See also Figure S1.

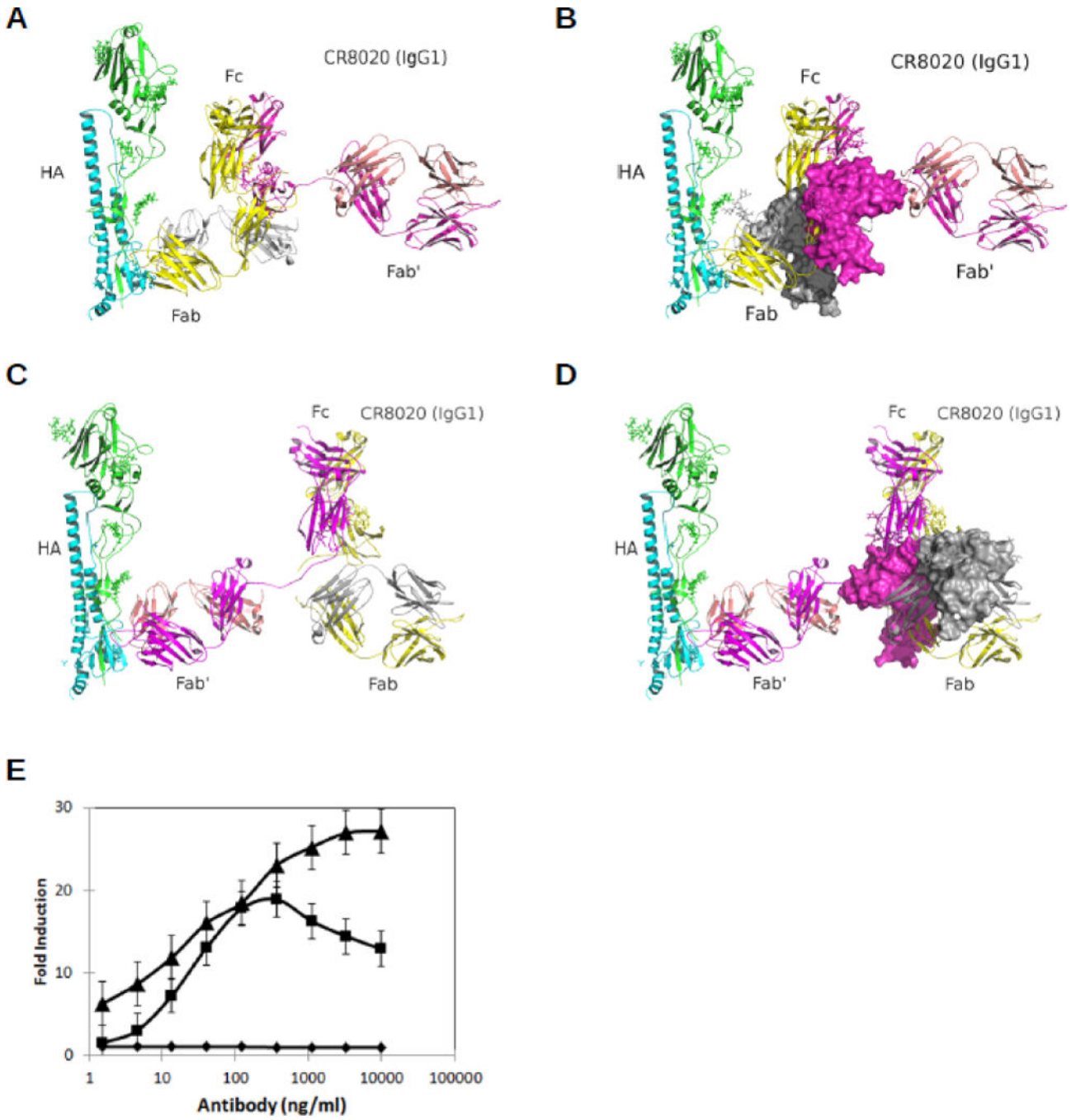

Figure 2. Modeling the HA-CR8020-FcγRIIa/HA-CR8020-FcγRIIIa activation complex and measurement of cell killing by anti-influenza antibodies

(A–D) The CR8020-HA complex crystal structure (PDB: 3SDY) was used to model the IgG-HA interaction. Given the different orientations of the two Fab domains (from here onward referred to as *Fab* and *Fab'*) with respect to the Fc, as observed in the human IgG1 X-ray crystal structure (PDB: 1HZH), two different IgG-HA models were constructed (METHODS) where, in one case, *Fab* was docked against the H3, and, in the other, *Fab'* was docked against the H3 **(A & C)**. Then, FcγRIIa and FcγRIIIa, represented by solvent

accessible surface and colored in gray and magenta, respectively, were docked against Fc in a fashion (METHODS) that mimics their interaction seen in the Fc:FcγRIIa (PDB: 3RY6) and Fc:FcγRIIa (PDB: 3AY4) co-crystal structures **(B & D)**. In the first model, the FcγRIIIa is proximal to the membrane, which could cause steric hindrance; interaction with FcγRIIa is sterically hindered by the membrane **(B)**, whereas, in the second model, the *Fab* domain is oriented too close to the viral membrane, which suggests that the model is not plausible **(C & D)**. (**E**) The ability for CR8020 (■) and an antibody targeting the trimeric interface (▲)to lyse influenza-infected A549 cells was measured. A IgG binding to an irrelevant antigen (◆) showed no activity in this assay. Results are shown as an average + standard error (n=3). See also Figures S2.

Table 1

Analysis of CR8020 epitope conservation in 3,794 human, avian and swine A/H3N2 HA sequences

At each site, the predicted escape mutations are ranked (>) according to difference in free energy of binding. Mutation potential was measured by applying SIN analysis on the crystal structure of A/X-31(H3N2) H3 (PDB: 1HGG).

HA2 Position (H3 numberin g)	Consens us	Alignment Details	Number of Sequences	SIN Score	Predicted escape mutations
15	Glu	Glu=3793,Lys=1	3,794	0.1596	A
16	Gly	Gly=3794	3,794	0	V > E > A
19	Asp	Asn=39,Asp=3753,Glu=1,Gly=1	3,794	0.1171	
25	Arg	Arg=3794	3,794	0.5316	
30	Glu	Glu=3793,Val=1	3,794	0.1586	A > D
32	Thr	Arg=1325,Ile=530,Met=13,Thr=1923, Val=3	3,794	0.0904	
33	Gly	Glu=3,Gly=3791	3,794	0	V > A > R
34	Gln	Gln=3794	3,794	0.4111	
35	Ala	Ala=3784,Val=10	3,794	0.0656	S
36	Ala	Ala=3794	3,794	0.0672	S
38	Leu	Arg=1,Ile=17,Leu=3764,Phe=12	3,794	0.1189	
146	Asn	Asn=3792,Asp=1,Val=1	3,794	0.2075	
150	Gly	Arg=1,Asp=6,Gln=1,Glu=275,Gly=350 9,Lys=1,Val=1	3,794	0.2677	

Table 2

Conservation of CR8020 epitope residues computed across 612 avian, human and swine H7 HA sequences and predicted escape mutations

At each site, the predicted escape mutations are ranked (>) according to difference in free energy of binding. Mutation potential was measured by applying SIN analysis on the crystal structure of A/Shanghai/02/2013(H7N9) HA (PDB: 4LN3).

HA2 position (H3 numbering)	Consensus	Alignment Details	Number of Sequences	SIN Score	Predicted escape mutations
15	Glu	Glu=612	612	0.1015	W > H > T
16	Gly	Gly=612	612	0	W > Q
19	Asp	Asn=98,Asp=514	612	0.0733	
25	Arg	Arg=604,Lys=8	612	0.3713	
30	Gln	Gln=612	612	0.113	T > S
32	Glu	Glu=609,Lys=3	612	0.1615	
33	Gly	Glu=1,Gly=611	612	0	L
34	Thr	Asn=1,Ile=13,Thr=598	612	0.1574	
35	Ala	Ala=612	612	0.0459	W
36	Ala	Ala=612	612	0.0246	N > K > Q > R > S > D
38	Tyr	His=1,Tyr=611	612	0.1735	
146	Asp	Asn=6,Asp=606	612	0.1509	
150	Ala	Ala=330,Glu=281,Gly=1	612	0.0468	S